

## ELECTRICAL CONDUCTIVITY, DIELECTRIC PERMITTIVITY AND DYNAMIC MECHANICAL PROPERTIES OF GRAPHENE/EPOXY NANOCOMPOSITES

J. WANG<sup>a</sup>, Y. JIN<sup>a</sup>, C. WANG<sup>a,b</sup>, Y. WANG<sup>a</sup>, Z. HAN<sup>a,b,\*</sup>

<sup>a</sup>*School of Material Science and Engineering, Harbin University of Science and Technology, Harbin, 150040, P.R. China*

<sup>b</sup>*Key Laboratory of Engineering Dielectrics and Its Application, Ministry of Education, Harbin University of Science and Technology, Harbin 150080, P. R. China*

Electrical conductivities, dielectric properties, dynamic mechanical behaviors of graphene/epoxy nanocomposites were investigated to understand the complex relationships among dielectric properties, frequency and graphene content. Dielectric origin was proposed according to the charge transport and dipole polarization by cole-cole fitting. As a result, the conductivity and permittivity of the nanocomposites presented percolation-dominated behaviors with a percolation threshold of 1.0 wt.% graphene. At percolation threshold, a dielectric permittivity of  $5.4 \times 10^3$  at 1 kHz and AC conductivity of  $1.04 \times 10^{-5}$  S/cm at 1 kHz were achieved, and the nanocomposites showed 17% higher storage modulus and 4 °C higher glass transition temperature than epoxy resin. The nanocomposites underwent dipolar polarization relaxation, the polar segments relaxation at the vicinity of graphene and the segmental relaxation restricted by graphene. Interfacial polarization contributed to the strong frequency dependence of the dielectric permittivity.

(Received July 9, 2018; Accepted October 12, 2018)

*Keywords:* Graphene, Epoxy, Dielectric permittivity, Electrical conductivity

### 1. Introduction

Polymer based composites with high dielectric permittivity have attracted much research attention due to their great potential applications in capacitors, actuators, electromagnetic interference shielding and so on [1,2]. Graphene, thanks to its intrinsic two-dimensional structure and unique electrical properties, has been regarded as an excellent filler to obtain high permittivity composites [3,4]. In the past decade, many efforts from both theoretical and experimental points of view have been made to investigate the dielectric properties of polymer composites with graphene and its derivatives including graphene oxide (GO), reduced graphene oxide (RGO) and exfoliated graphite nanoplatelets (xGnP) [5,6]. A high dielectric permittivity shooting up to  $10^7$  at 1 kHz was achieved by adding 2.34 vol.% xGnP into poly(vinylidene fluoride) (PVDF) [7]. A permittivity of 1875 at 1 kHz was obtained by adding 2 vol.% thermally RGO into thermoplastic polyurethanes

---

\* Corresponding author: zhidong.han@hrbust.edu.cn

(TPU) [8]. A permittivity of 600 at 1 kHz was reported by adding 3 wt.% graphene into epoxy resin [9]. GO, rather than graphene, was usually adopted to obtain epoxy based composites of high permittivity on account of its good compatibility and versatile modification [10,11]. As an example, epoxy composites filled with 1.0 wt.% RGO functionalized with diglycidyl ether of bisphenol-A had a dielectric permittivity of 32 at 1 kHz [12].

The giant increment in the dielectric permittivity of graphene based composites was frequently explained by the percolation theory, the micro-capacitor model, and the Maxwell-Wagner-Sillars (MWS) effect [6,7,13,14], among which the percolation theory has been widely investigated. The percolation threshold represents a critical filler content at which continuous conduction network comes into form throughout the matrix [1]. Several methods have been reported to build the percolation structure by improving the dispersion of graphene in polymeric matrix, which is crucial to decrease the percolation threshold. Tian et al. [15] reported a percolation threshold of 0.25 vol.% by encapsulating GO with carboxylated nitrile rubber latex. Shang et al. [16] reported a percolation threshold of 1.29 vol.% by orienting graphene in PVDF. He et al. [7] reported a percolation threshold of 1.01 vol.% by ultrasonically mixing xGnP with PVDF solution.

The percolation dominated conductivity and permittivity showed strong dependence on the microstructure of graphene and the interactions between graphene and polymeric matrix [9,13]. Graphene was reported to affect macromolecular mobility and interfacial structure [8,17], which altered the dielectric relaxations and the dielectric permittivity of the composites. The two-dimensional structure and the high aspect ratio of graphene also contributed to the formation of microcapacitor [7,13,18], which was considered to be one of the fundamental factors in determining the permittivity of the composites. On the other hand, the complex structures and the diverse permittivities of graphene and its derivatives were also the reasons that caused the great deviation of dielectric properties reported in the literatures [19,20]. Hereinafter, attempts were made to understand the origins of the frequency dependent permittivity of graphene/epoxy nanocomposites. The influences of the microstructure of graphene/epoxy composites and the interactions between graphene and epoxy matrix on the dielectric and mechanical behaviors were investigated according to the results from morphology, conductivity, permittivity, and glass transition temperature. The dielectric relaxation was studied and proposed according to the charge transport and dipole polarization by cole-cole fitting of the real and imaginary dielectric permittivity.

## 2. Experimental

Graphene/epoxy nanocomposites were prepared with epoxy resin (JY-257, Changshu Jiafa Chemical Co. Ltd.) and graphene nanoplatelets (GNP, 2-3 layers, Guangzhou Hongwu Material Technology Co. Ltd.). A solvent-assisted method was adopted to improve the dispersion of GNP. Accordingly, GNP was dispersed in ethanol with ultrasonic treatment for 15 min, and then mixed with epoxy resin for 15 min by ultrasonication. The solution was kept at 60 °C under vacuum to remove the solvent. Amine based curing agent (593, Wuxi Resin Factory of BlueStar New Chemical Materials Co. Ltd.) was added into the degassed solution at 15 wt.% dosage of epoxy. The curing was performed at 80°C for 5 h and post-curing at 100°C for 6 h. The samples were

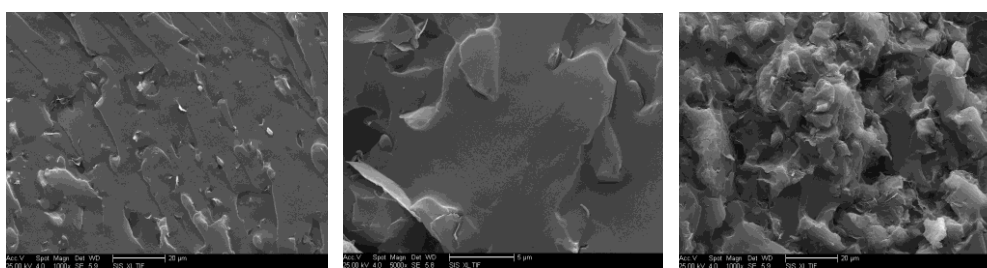
labeled as EP-GNP<sub>x</sub>, where x (0.2, 0.5 and 1.0, respectively) represented the weight content of GNP.

Morphological structure of nanocomposites was observed by scanning electron microscopy (SEM, FEI Sirion-200). The cryofractured surface of sample was metalized with gold. Dynamic mechanical thermal analysis (DMA) was performed in tensile mode at 1 Hz using a Dynamic Mechanical Analyzer (Q-800, TA). Samples with the width of 4.0 mm and the thickness of 0.5 mm were tested at a heating rate of 2 °C/min from 30 to 200 °C in air atmosphere. Broadband dielectric spectroscopy (Alpha-A, Novocontrol) was used for dielectric analysis in the frequency range from 1 Hz to 10<sup>6</sup> Hz on the samples with diameter of 40 mm and thickness of 1 mm. Aluminum electrodes with the diameter of 25 mm were electroplated on the surface of the sample. Direct current (DC) volume resistivity of graphene/epoxy nanocomposites were measured by a resistivity meter (ZC-90G, Taiou Electronics).

### 3. Results and discussion

#### 3.1. Morphological structure

The dispersion of graphene in epoxy matrix is crucial to determine the final performance of graphene/epoxy nanocomposites [ 21 ]. Fig.1 shows the morphological structure of graphene/epoxy nanocomposites. Graphene nanoplatelets are found to be well dispersed in the epoxy matrix for the nanocomposites with 0.2 wt.% graphene. Good adhesion of graphene to the matrix is observed. As the content of graphene increased to 0.5 wt.%, more nanoplatelets appeared in the observing view. Graphene nanoplatelets still showed good dispersion, and some connections were found between the neighbour nanoplatelets. For the nanocomposites with 1.0 wt.% graphene, the aggregation of nanoplatelets could be obviously observed. Nanoplatelets were stacked to form larger plates and epoxy resin was observed between the interplate space. As the content of graphene increases, the cryofractured surface of the nanocomposites changes from smooth morphology to rough status.



(a) graphene-0.2%

(b) graphene-0.5%

(c) graphene-1.0%

*Fig. 1. SEM micrographs of graphene/epoxy nanocomposites with the graphene content of 0.2 wt.%(a), 0.5 wt.%(b) and 1.0 wt.%(c), respectively.*

#### 3.2. Dynamic mechanical properties

Fig. 2 shows the dynamic mechanical properties of epoxy resin and its nanocomposites with graphene. The graphene/epoxy nanocomposites show enhanced storage modulus before glass

transition, among which the storage modulus of the nanocomposites with 1.0 wt.% graphene is about 17% higher than that of epoxy resin. The nanocomposites start the glass transition at lower temperature than epoxy, and then the storage modulus decreases sharply. The glass transition temperature ( $T_g$ ) of the nanocomposites, corresponding to the peak temperature of loss tangent, goes up as the graphene content increases.

The glass transition of the nanocomposites can be influenced by graphene mainly in two ways [22]. One is the decreased curing degree with addition of graphene, and the other is the restricted segmental motion by graphene layers. The former leads to a drop in  $T_g$  and the latter to a rise. When the graphene content is low, the restriction effect of graphene layers is weak. However, the influence of graphene on the curing degree of epoxy resin is ineluctable due to its interactions with the epoxy components and its thermophysical effects [17,21]. Consequently,  $T_g$  of the nanocomposites with 0.2 wt.% graphene is about 8 °C lower than that of epoxy resin. As graphene content increases, the restriction effect becomes ascendant, which makes more contribution to the rise of  $T_g$ . The nanocomposites with 0.5 and 1.0 wt.% graphene show  $T_g$  about 4 and 12 °C higher than that of the nanocomposites with 0.2 wt.%, respectively.

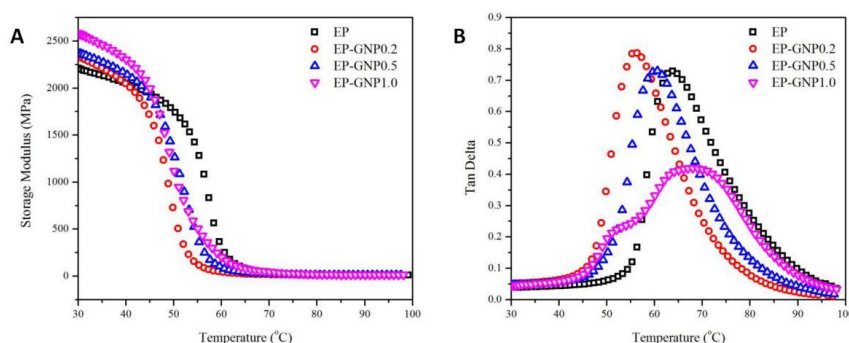


Fig. 2. Dynamic mechanical properties of epoxy resin and its nanocomposites with different loading of graphene. (a) Storage modulus versus temperature curves; (b)  $Tan(\Delta)$  versus temperature curves.

The glass transition of nanocomposites is greatly influenced by the dispersion of graphene in epoxy matrix. At high graphene content, the aggregation and the poor dispersion of graphene were reported to lower  $T_g$  and widen the transition peak [23,22]. As shown in Fig. 2, a shoulder peak appears at low temperature side of loss tangent peak of the nanocomposites with 1.0 wt.% graphene. Such phenomena can be interpreted by the inhomogeneous distribution of graphene in the nanocomposites, as confirmed in Fig. 1. According to the peak temperature, the low and high  $T_g$  can be basically assigned to graphene-poor and graphene-rich regions, respectively. The heterogeneous graphene distribution will affect dielectric relaxation [22-24].

### 3.3. Electrical conductivity

Fig. 3a presents the frequency dependence of real conductivity ( $\sigma'$ ) of epoxy resin and graphene/epoxy nanocomposites with different loading of graphene.  $\sigma'$  is found to increase with the AC frequency for all the samples, and  $\sigma'$  of the nanocomposites with 1.0 wt.% graphene is much higher than other materials. The curve of EP-GNP1.0 is distinct from other curves by

showing a plateau from 1 to  $10^3$  Hz, which indicates the formation of conductive network.  $\sigma'$  at  $10^3$  Hz as a function of the graphene loading is shown in Fig. 3b together with the DC conductivity. The conductivities of the nanocomposites slightly increase with graphene content when the graphene content is lower than 0.5 wt.%, and then great leap in several orders of magnitude is observed as graphene content increases from 0.5 to 1.0 wt.%. Accordingly, the percolation threshold at 1.0 wt.% can be proposed. Similar percolation threshold of graphene/epoxy nanocomposites was reported by Monti et al. [23].

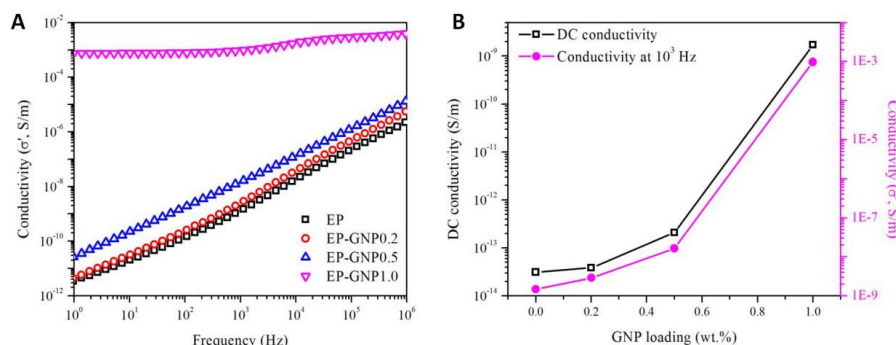


Fig. 3. Electrical conductivity of epoxy resin and its nanocomposites with different loading of graphene. (a) Real conductivity versus frequency curves; (b) DC conductivity and real conductivity at  $10^3$  Hz versus graphene loading curves.

The addition of graphene to epoxy resin enhances the electrical conduction due to the electronic contribution along the networks of graphene [24]. The conductivities in the low frequency range are mainly controlled by the static effects and depend on the content of graphene [6]. As seen in Fig. 3a, the percolation effect is significant at low frequency, resulting in a seven-order increase of  $\sigma'$  at 1 Hz. As frequency increases, the electron hopping becomes predominant, leading to the less difference due to the graphene loading.

### 3.4. Dielectric permittivity

Fig. 4a shows the frequency dependence of the real permittivity ( $\epsilon'$ ) of epoxy resin and its nanocomposites with graphene.  $\epsilon'$  is greatly influenced by the graphene content and the frequency. In the low frequency range, the differences among the curves are significant, and the percolation effect can be obviously observed when graphene content is 1.0 wt.%. When graphene content is lower, the MWS effect is weak due to the large distance between graphene layers and  $\epsilon'$  slightly increases with the graphene loading from 0.2 to 0.5 wt.%. At the percolation threshold, large amounts of charges accumulate at the interface and  $\epsilon'$  increases remarkably over  $10^4$  at 1 Hz. As the frequency increases, the charges accumulated at the interface reduce dramatically, and thus  $\epsilon'$  displays a sharp decrease from  $10^4$  at 1 Hz to  $10^2$  at  $10^5$  Hz.

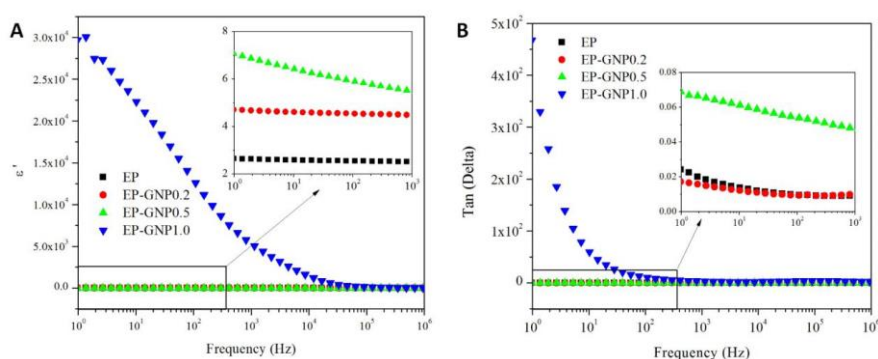


Fig. 4. Dielectric properties of epoxy resin and its nanocomposites with different loading of graphene. (a) Real permittivity ( $\epsilon'$ ) versus frequency curves; (b) Loss tangent ( $\tan\delta$ ) versus frequency curves.

The large dielectric mismatch between graphene and epoxy resin leads to the entrapment of charges at the interfaces [6,13]. MWS effects play predominant role in determining the permittivity of nanocomposites in the low frequency range, which is characteristic of the frequency dependence of the dielectric permittivity. As frequency increases, the accumulated charges are conducted through interface, leading to the decrease of the dielectric permittivity at high frequency [6]. Meanwhile, microcapacitors composed of graphene and epoxy also make contributions to the permittivity in the high frequency range [7]. An abrupt increase of loss tangent happens at the percolation threshold owing to the formation of conductive network, as seen in Fig. 4b. The dielectric loss tangent of the nanocomposites with 1.0 wt.% decreases by two orders of magnitude as the frequency increases from 1 to 10<sup>3</sup> Hz.

### 3.5. Dielectric relaxation

Fig. 5 plots  $\epsilon'$ - $\epsilon''$  curves of epoxy and graphene/epoxy nanocomposites. For epoxy resin, the permittivity is controlled by the number of orientable dipoles and their ability to orient under an applied electric field [25].  $\epsilon''$  decreases as  $\epsilon'$  increases in the high frequency range, and the curve is vaulted. The  $\epsilon'$ - $\epsilon''$  curve of the nanocomposites with 0.2 wt.% graphene changes into the shape with two arcs. The small left arc in the high frequency range indicates the relaxation from the polar segments at the vicinity of graphene, while the right arc justifies the dipolar relaxation of epoxy resin. The line in the low frequency region is greatly intensified for the nanocomposites with 0.5 wt.% graphene, which reveals the enhanced conductance relaxation due to interfacial polarization. The two arcs in the high frequency range represent the relaxations from the restricted epoxy segments and the polar segments at the vicinity of graphene. As the graphene content is 1.0 wt.%, the relaxations are mainly from the restricted epoxy segments and MWS polarization since the charges can be conducted along the percolation structure and the conductance reaches a very high level.

Dielectric spectroscopy provides the information of the dielectric relaxations under applied AC field. The dielectric absorption originated from Debye polarization in relative high frequency range can be viewed as simple relaxation process, which can be fitted quite well with the Cole-Cole equation.

$$\varepsilon^* = \varepsilon_\infty + \frac{\varepsilon_s - \varepsilon_\infty}{1 + (i\omega\tau)^{1-\alpha}}$$

where  $\varepsilon^*$  is the complex dielectric constant,  $\varepsilon_s$  and  $\varepsilon_\infty$  are the dielectric constants at the static and infinite frequency,  $\omega$  is the angular frequency and  $\tau$  is a generalized relaxation time of certain polarization.  $\alpha$  is the exponent parameter which takes a value between 0 and 1.

Fitting results by the cole-cole equation show the dielectric permittivity and relaxation time in Table 1. The dipolar polarization of EP can keep pace with the frequency change of external electric field due to the short relaxation time. Accordingly, the permittivity of epoxy keeps nearly constant at high frequency. With addition of 0.2 wt.% graphene, the relaxation time of the same magnitude order reveals the free dipolar polarization of epoxy segments. When the graphene content increases further to 0.5 and 1.0 wt.%, the relaxation time increases by two orders of magnitude, which demonstrates the increased rigidity as the segmental motion is restricted by graphene.

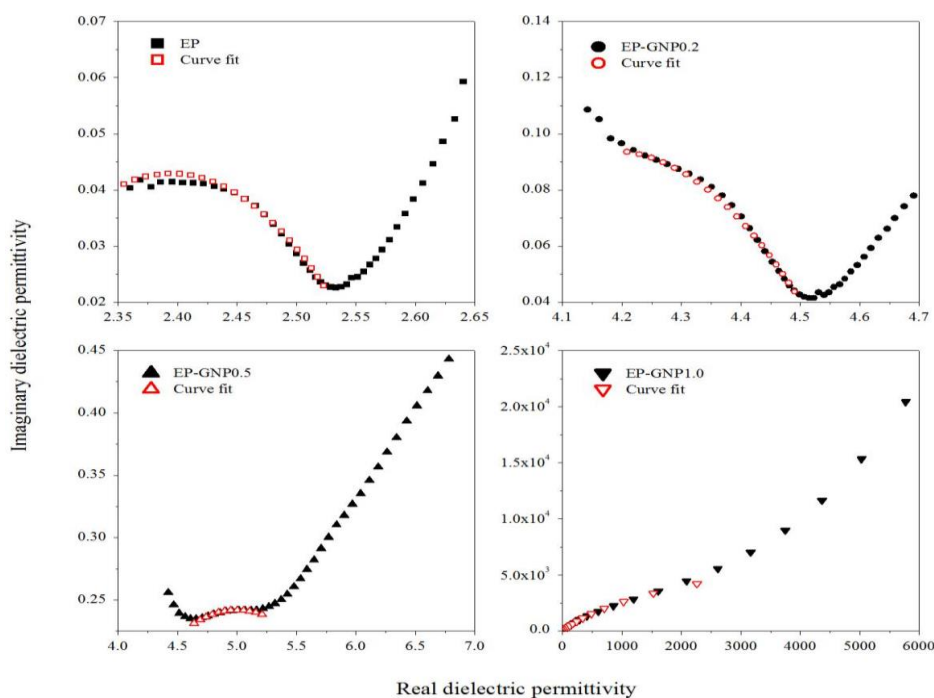


Fig. 5. Complex dielectric permittivity curves of (a) epoxy resin and its nanocomposites with (b) 0.2, (c) 0.5 and (d) 1.0 wt.% graphene.

As graphene content increases, the dielectric relaxation of the nanocomposites undergoes three different stages, which are dipolar relaxation, the polar segments relaxation at the vicinity of graphene and the segmental relaxation restricted by graphene. Interfacial polarization in heterogeneous systems leads to the frequency dependence of the dielectric permittivity in the low frequency range. As frequency increases, the frequency-affected electron hopping and dipolar relaxation start to take over. Meanwhile, the disparity between the conductivities of graphene and epoxy resin will cause the formation of microcapacitors. At percolation threshold, the nanocomposites presents a resistive behavior at low frequencies (plateau) and capacitive at high frequencies [26].

Table 1. Parameters derived from the Cole-Cole fitting for epoxy and graphene/epoxy nanocomposites.

Sample	$\epsilon_{\infty}$	$\epsilon_s$	$\tau$ (s)
EP	2.21	2.58	$7.94 \times 10^{-8}$
EP-GNP0.2	3.76	4.60	$1.00 \times 10^{-8}$
EP-GNP0.5	3.30	6.70	$1.25 \times 10^{-6}$
EP-GNP1.0	9.20	16800	$1.03 \times 10^{-6}$

#### 4. Conclusions

The electrical conductivity, dielectric permittivity and storage modulus were enhanced as graphene content increased. A percolation threshold was proposed to be 1.0 wt.%, at which a dielectric permittivity of  $5.4 \times 10^3$  and AC conductivity of  $1.04 \times 10^{-5}$  S/cm at 1 kHz were achieved. The nanocomposites with graphene content lower than percolation threshold presented lower  $T_g$  than epoxy resin, and the nanocomposites at percolation threshold had about 4 °C higher  $T_g$ . Furthermore, the aggregation and inhomogeneous distribution of graphene were evidenced by the shoulder peak at low temperature side when the graphene content is 1.0 wt.%. Morphological investigation of nanocomposites with different graphene contents by SEM evidenced the structure of microcapacitor with epoxy resin between two nanoplatelets, interconnection among the nanoplatelets and continuous networks by overlapping of nanoplatelets. Interfacial polarization gave rise to the frequency dependence of the dielectric permittivity in the low frequency range, while the frequency-affected electron hopping and dipolar relaxation acted in the high frequency range. Fitting by Cole-Cole equation, the restricted dipolar polarization with longer relaxation time was determined. The dielectric relaxation of the nanocomposites underwent dipolar polarization relaxation, the polar segments relaxation at the vicinity of graphene and the segmental relaxation restricted by graphene.

#### Acknowledgements

The authors would like to thank Dr. Jiaming Yang for his help in the analysis of dielectric spectroscopy.

#### Funding

This work was supported by the Science Fund for Distinguished Young Scholars of Heilongjiang Province [JC201312]; the Harbin Technological Innovation Fund for Distinguished Young Scholars [2014RFYXJ009]; the Program for Innovative Research Team in University of Heilongjiang Province [2013TD008]; the Project of Key Laboratory of Engineering Dielectrics and Its Application [DE2012B04]; Natural Science Foundation of Heilongjiang Province (E2018040); and the Project of National Natural Science Foundation of China [50802022].

## Declaration of Conflicting Interests

The authors declare that there is no conflict of interest.

## References

---

- [1] Z. Dang, J. Yuan, J. Zha, et al. *Prog. Mater. Sci.* **57**, 660 (2012).
- [2] H. Tang, G. Chen, Q. Li, *Mater. Lett.* **184**, 143 (2016).
- [3] M. Haneef, H. Saleem, A. Habib, *Synthetic Met.* **223**, 101 (2017).
- [4] A. C. Patsidis, K. Kalaitzidou, G. C. Psarras, *Mater. Chem. Phys.* **135**, 798 (2012).
- [5] D. J. Mowbray, *Phys. Status Solidi B* **251**, 2509 (2014).
- [6] X. Xia, Y. Wang, Z. Zhong, et al., *Carbon* **111**, 221 (2017).
- [7] F. He, S. Lau, H. L. Chan, et al., *Adv. Mater.* **21**, 710 (2009).
- [8] S. Liu, M. Tian, B. Yan, et al., *Polymer* **56**, 375 (2015).
- [9] H. Wei, Y. Zhang, H. Zhang, et al., *High Perform. Polym.* **27**, 911 (2015).
- [10] R. Wang, D. Zhuo, Z. Weng, et al., *J. Mater. Chem. A* **3**, 9826 (2015).
- [11] K. Deshmukh, M. B. Ahamed, K. K. Sadasivuni, et al., *Mater. Chem. Phys.* **186**, 188 (2017).
- [12] Y. Wan, W. Yang, S. Yu, et al., *Compos. Sci. Technol.* **122**, 27 (2016).
- [13] M. Tian, Z. Wei, X. Zan, et al., *Compos. Sci. Technol.* **99**, 37 (2014).
- [14] X. Xu, C. Yang, J. Yang, et al., *Compos. Part B Eng.* **109**, 91 (2017).
- [15] M. Tian, J. Zhang, L. Zhang, et al., *J. Colloid. Interf. Sci.* **430**, 249 (2014).
- [16] J. Shang, Y. Zhang, L. Yu, et al., *Mater. Chem. Phys.* **134**, 867 (2012).
- [17] T. K. Sharmila, A. B. Nair, B. T. Abraham, et al., *Polymer* **55**, 3614 (2014).
- [18] F. He, K. Lam, J. Fan, et al., *Carbon* **80**, 496 (2014).
- [19] E. Santos, E. Kaxiras, *Nano Lett.* **13**, 898 (2013).
- [20] K. S. Kumar, S. Pittala, S. Sanyadanam, et al., *RSC Adv.* **5**, 14768 (2015).
- [21] Y. Wan, L. Tang, D. Yan, et al., *Compos. Sci. Technol.* **82**, 60 (2013).
- [22] L. Tang, Y. Wan, D. Yan, et al., *Carbon* **60**, 16 (2013).
- [23] M. Monti, M. Rallini, D. Puglia, et al., *Compos. Part A* **46**, 166 (2013).
- [24] Z. M. Elimat, *J. Compos. Mater.* **49**, 3 (2015).
- [25] B. Wang, L. Liu, L. Huang, et al., *Carbon* **85**, 28 (2015).
- [26] W. Bauhofer, J. Z. Kovacs, *Compos. Sci. Technol.* **69**, 1486 (2009).